Title
KLF12 Regulates Mouse NK Cell Proliferation.

Journal
The Journal of Immunology, 203(4)

ISSN
0022-1767

Authors
Lam, Viola C
Folkersen, Lasse
Aguilar, Oscar A
et al.

Publication Date
2019-08-15

DOI
10.4049/jimmunol.1900396

Peer reviewed

The Journal of Immunology

KLF12 Regulates Mouse NK Cell Proliferation

Viola C. Lam, Lasse Folkersen, Oscar A. Aguilar and Lewis L. Lanier

J Immunol published online 12 July 2019
http://www.jimmunol.org/content/early/2019/07/11/jimmunol.1900396

Supplementary Material **http://www.jimmunol.org/content/suppl/2019/07/11/jimmunol.1900396.DCSupplemental**

The Journal of Immunology is published twice each month by
The American Association of Immunologists, Inc.,
1451 Rockville Pike, Suite 650, Rockville, MD 20852

Print ISSN: 0022-1767 Online ISSN: 1550-6606.

Published July 12, 2019, doi:10.4049/jimmunol.1900396

KLF12 Regulates Mouse NK Cell Proliferation

Viola C. Lam,*,† Lasse Folkersen,‡ Oscar A. Aguilar,†,§ and Lewis L. Lanier†,§

NK cells are innate lymphocytes that play an integral role in tumor rejection and viral clearance. Unlike their other lymphocyte counterparts, NK cells have the unique ability to recognize and lyse target cells without prior exposure. However, there are no known NK cell-specific genes that are exclusively expressed by all NK cells. Therefore, identification of NK cell-specific genes would allow a better understanding of why NK cells are unique cytotoxic lymphocytes. From the Immunological Genome (ImmGen) Consortium studies, we identified kruppel-like factor 12 (*Klf12*), encoding a novel transcription factor, preferentially expressed in C57BL/6 mouse NK cells. KLF12 was dispensable for NK cell development, IFN-γ production, degranulation, and proliferation in *Klf12* knockout mice. RNA-sequencing analysis revealed increased expression of *Btg3*, an antiproliferative gene, in KLF12-deficient NK cells compared with wild-type NK cells. Interestingly, competitive mixed bone marrow chimeric mice exhibited reduced development of KLF12-deficient NK cells, altered IFN-γ production and degranulation, and impairment of NK cell proliferation in vitro and in vivo in response to mouse CMV infection. KLF12-deficient NK cells from bone marrow chimeric mice also expressed higher levels of the IL-21R, which resulted in increased IL-21R signaling and correlated with greater inhibition of NK cell proliferation. Furthermore, IL-21 induced *Btg3* expression, which correlated with arrested NK cell maturation and proliferation. In summary, we found that KLF12 regulates mouse NK cell proliferation potentially by regulating expression of *Btg3* via IL-21. *The Journal of Immunology*, 2019, 203: 000–000.

Patients with genetic mutations resulting in diminished NK cell numbers or function succumb to recurrent herpesvirus and papillomavirus infections (1–4), highlighting the importance of NK cells in controlling certain viral infections. NK cells are cytotoxic lymphocytes that have the unique ability to recognize and lyse target cells without prior exposure. NK cells also secrete cytokines, such as IFN-γ, to activate other immune cells to coordinate appropriate immune responses against pathogens (5).

Mouse CMV (MCMV) infection is an ideal model to study NK cell activation, expansion, and effector function. At the onset of infection, IL-12 production by dendritic cells is critical for early NK cell production of IFN-γ and control of viral load (6–8). A subset of NK cells expressing the activating Ly49H$^+$ receptor in C57BL/6 mice specifically recognizes the MCMV-encoded glycoprotein, m157 (9, 10). Ly49H$^+$ NK cells expand, contract, and persist after MCMV infection (11). These cells conferred specific protection against MCMV rechallenge and not other heterologous infections, indicating that these are MCMV-specific memory NK cells (12, 13).

NK cells share expression of many genes with their lymphocyte counterparts; therefore, we sought to find genes preferentially expressed by NK cells in the hematopoietic cell lineage to understand their unique activation and cytotoxic capabilities. From the Immunological Genome (ImmGen) Consortium, we identified kruppel-like factor 12 (KLF12), a novel transcription factor, to be preferentially expressed in mouse NK cells. KLF12 is a zinc finger transcription factor in the Kruppel-like factor family. Similar to KLF3 and KLF8, KLF12 has a conserved PVDLS domain at the N terminus that binds to the corepressor, CtBP1 (14–16). *Klf12* transcripts are found in the kidney, endometrial stromal cells, primary gastric tumors, and various cancer cell lines (15, 17–19). Prior studies have demonstrated that KLF12 binds to a conserved CACCC sequence and functions as a transcriptional repressor or activator, suggesting that the function of KLF12 is context and cell type specific (17, 20, 21). KLF12 target genes are largely unknown but include *NR4A1* (Nur77), *TRAP2A*, *FOXO1*, *SLC14A2*, and *EGR1* (17, 20, 22–25).

In this study, we assessed the role of KLF12 in mouse NK cells as a potential transcriptional regulator of NK cell development and/or effector functions. To address this, we generated a mouse with floxed *Klf12* loci and crossed these the mice expressing β-actin Cre recombinase to delete KLF12 expression. We assessed the development, proliferation, and effector functions of KLF12-deficient NK cells in response to in vitro stimulation and MCMV infection.

Materials and Methods

Mice

Mice were obtained from the following sources: wild-type (WT) C57BL/6 and C57BL/6 CD45.1 mice were purchased from the National Cancer Institute (Frederick, MD), *Rosa26-Flippase* C57BL/6 mice from Dr. R. Locksley and *β-actin Cre* transgenic C57BL/6 mice from Dr. M. McManus, University of California San Francisco (UCSF), and *Klra8*$^{-/-}$ (Ly49H-deficient) C57BL/6 mice from Dr. S. Vidal, McGill University. The *Klf12* targeting vector was

*Biomedical Sciences Graduate Program, University of California San Francisco, San Francisco, CA 94143; †Department of Microbiology and Immunology, University of California San Francisco, San Francisco, CA 94143; ‡Sankt Hans Hospital, Capital Region Hospitals, DK 2000 Copenhagen, Denmark; and §Parker Institute for Cancer Immunotherapy, San Francisco, CA 94129

ORCIDs: 0000-0003-0708-9530 (L.F.); 0000-0003-1308-3952 (L.L.L.).

Received for publication April 4, 2019. Accepted for publication June 17, 2019.

This work was supported by National Science Foundation Grant Graduate Research Fellowship Program 1650113, National Institutes of Health Grant T32AI007334 (to V.C.L.), and National Institutes of Health Grant AI068129 (to L.L.L.).

Address correspondence and reprint requests to Dr. Lewis L. Lanier, Department of Microbiology and Immunology, University of California San Francisco, 513 Parnassus HSE 1001G, San Francisco, CA 94143-0414. E-mail address: Lewis.Lanier@ucsf.edu

The online version of this article contains supplemental material.

Abbreviations used in this article: BM, bone marrow; DN, double negative; DP, double positive; gDNA, genomic DNA; ILC, innate lymphoid cell; ImmGen, Immunological Genome; KLF12, kruppel-like factor 12; MCMV, mouse CMV; MFI, mean fluorescence intensity; rh, recombinant human; rm, recombinant mouse; RNA-Seq, RNA sequencing; UCSF, University of California San Francisco; WT, wild-type.

purchased from the International Mouse Knockout Consortium and electroporated into E14-129/Ola embryonic stem cells. Selected clones were then microinjected into C57BL/6 females, and heterozygotes were backcrossed at least nine generations onto the C57BL/6 background. *Klf12*-floxed mice were genotype by PCR using the following primer pairs: WT, forward, 5′-CACAGCGAGTTCCCCAAGAT-3′, reverse 1, 5′-GGACGCACATACAGCTTCCT-3′, reverse 2, 5′-AGGGAAAGGGTCGAGAGACA-3′; Flox, forward, 5′-CACAGCGAGTTCCCCAAGAT-3′, reverse 3, 5′-TAGGAGGTGTGGCTTTGCTG-3′, reverse 4, 5′-CCCTTTGTTGTCCGCCTACT-3′. Mice were bred and housed in a specific pathogen-free facility and experiments were performed according to UCSF Institutional Animal Care and Use Committee and National Institutes of Health guidelines.

Quantitative PCR

Total RNA from splenocytes or indicated cellar populations was prepared using the Ambion RNAqueous kit and converted into cDNA. Quantitative PCR analysis with SYBR Green master mix (Roche) was performed on the cDNA following standard conditions with the following primer pairs: *Klf12*, forward, 5′-CTGGCGAACCACATAGGCCCAG-3′, reverse, 5′-CGGCGGCCTACATTTACGTGAT-3′, *Btg3*, forward, 5′-TGCTGCCGGTATGGAGAGAA-3′, reverse, 5′-GGTCACCTTATCCAGAGCCC-3′; *Hprt*, forward, 5′-CACAGGACTAGAACACCTGC-3′, reverse, 5′-GCTGGTGAAAAGGACCTCT-3′. Primer pairs to confirm disrupted *Klf12*: *Klf12* exons 2-3, forward, 5′-GCTAATGCTTGATGGAATGCC-3′, reverse, 5′-AGTTGTGGACGTTTGGAGAC-3′; exons 5-6, forward, 5′-ACATCCATCCCCGGTATCCA-3′, reverse, 5′-TGGCGTCTTGTGCTCTCAAT-3′. Expressions were normalized to HPRT.

Southern blot and long range PCR

Genomic DNA (gDNA) from selected stem cell clones was processed using the Promega Wizard gDNA purification kit. gDNA was digested overnight with EcoRV, transferred onto a membrane, probed with α-^{32}P dATP against the 5′ arm of the *Klf12* targeting vector, and exposed to film. Probes were amplified using the following primer pair: forward, 5′-TCTCCCTCTTGGTGGTCACT-3′, reverse, 5′-GATGCCTGAAAACCGCACAG-3′. The 3′ arm of the targeting vector was amplified by PCR using Takara PrimeSTAR GXL DNA polymerase with the following primers: forward, 5′-GGATCTCATGCTGGAGTTCTTCGCC-3′, reverse 1, 5′-CCAAAGCCCCTATACCCTTCCCCGC-3′, and reverse 2, 5′-ATCTGGCGTGGGCGGCCAGCAGTTC-3′.

Ex vivo NK cell stimulations and proliferation assays

Splenocytes were resuspended in RPMI 1640 supplemented with 10% FCS, 50 μM 2-ME, 100 μM nonessential amino acids, 1 mM sodium pyruvate, 50 mM HEPES, and 2 μM L-glutamine. One million cells were stimulated for 6 h in the presence of BD GolgiStop with 20 ng/ml recombinant mouse (rm) IL-12 (no. 419-ML/CF; R&D Systems) and 10 ng/ml rmIL-18 (no. B0025; R&D Systems), with 20 ng/ml PMA and 200 ng/ml ionomycin or with 10 μg/ml of plate-bound anti-NK1.1 Ab (clone PK136), were fixed and permeabilized with BD Cytofix/Cytoperm and then stained for IFN-γ and CD107a. For p-STAT5 (no. 612599; BD Biosciences) and p-STAT3 (no. 557814; BD Biosciences) staining, 1 million cells were stimulated for the indicated times and concentrations with recombinant human (rh) IL-15 (no. 247-ILB; R&D Systems) or rmIL-21 (ZymoGenetics), fixed with 1% paraformaldehyde in PBS, permeabilized with methanol, and stained. For proliferation assays, 1 million CellTrace Violet (no. C34557; Invitrogen)–labeled splenocytes were cultured in 10 ng/ml rhIL-15, 1×10^5 paraformaldehyde-fixed RMA lymphoma cells, or MCMV m157–transduced RMA cells supplemented with 50 U/ml rhIL-2 (National Cancer Institute Preclinical Repository) or 100 ng/ml rmIL-21.

Bone marrow chimeras

Donor bone marrow (BM) was isolated from femurs and tibias of 8- to 10-wk-old WT and *Klf12*$^{F/F}$ C57BL/6 mice and mixed 1:1 in sterile PBS, and 5×10^6 cells were injected i.v. into WT recipients lethally irradiated with 1200 Gy. Recipient mice were injected i.p. with 200 μg anti-CD4 (GK1.5), 200 μg anti-CD8 (2.43), and 100 μg anti-NK1.1 (PK136) depleting Abs at the time of transfer and maintained on antibiotic pellets (S0443; Bio-Serv) for 2 wk. Recipients reconstituted for at least 8 wk were used for experiments.

NK cell enrichment and adoptive transfer

NK cells were enriched from spleens using mAbs against Ter119, Gr-1, CD4, CD8, CD19, and CD5. Qiagen anti-rat IgG magnetic beads were used to deplete the indicated populations. Enriched NK cells from WT or KLF12-deficient mice for adoptive transfer were mixed 1:1 and injected i.v. into Ly49H-deficient C57BL/6 recipients 1 d prior to MCMV infection.

MCMV infection and viral titers

Mice were injected i.p. with 1×10^4 PFU or 2.5×10^3 PFU of Smith strain MCMV for adoptive NK cell transfer experiments. For MCMV quantitation, oral lavage was collected by washing the sublingual cavity with sterile saline solution and used directly in quantitative PCR analysis (26). DNA was isolated from blood using a ReliaPrep Blood gDNA Miniprep System kit (Promega) and 1 μl was used for quantitative PCR analysis. MCMV primer pairs: forward, 5′-AGCCACCAACATTGACCACGCAC-3′ and reverse, 5′-GCCCCAACCAGGACACACAACTC-3′.

RNA sequencing

Total RNA from 6-wk-old *Klf12*$^{+/+}$ and *Klf12*$^{F/F}$ *β-actin Cre*$^-$ littermate males was isolated from CD3$^-$NK1.1$^+$ NK cells, CD4$^+$TCRβ$^+$CD25$^-$ T cells, CD8$^+$TCRβ$^+$CD25$^-$ T cells and B220$^+$IgM$^+$IgD$^+$ B cells following the ImmGen standard protocol (https://www.immgen.org/). One thousand cells (≥99% purity) were double sorted directly into 96-well plates containing TCL buffer (Qiagen) and 1% 2-ME, frozen, and analyzed by the Broad Technology Labs for SmartSeq2 library preparation and NextSeq500 sequencing. Transcripts were quantified using Cuffquant and then normalized using DEseq (27–31). Raw data were interpreted by Database for Annotations, Visualization and Integrated Discovery (DAVID), analyzing all differentially expressed genes using default parameters (32).

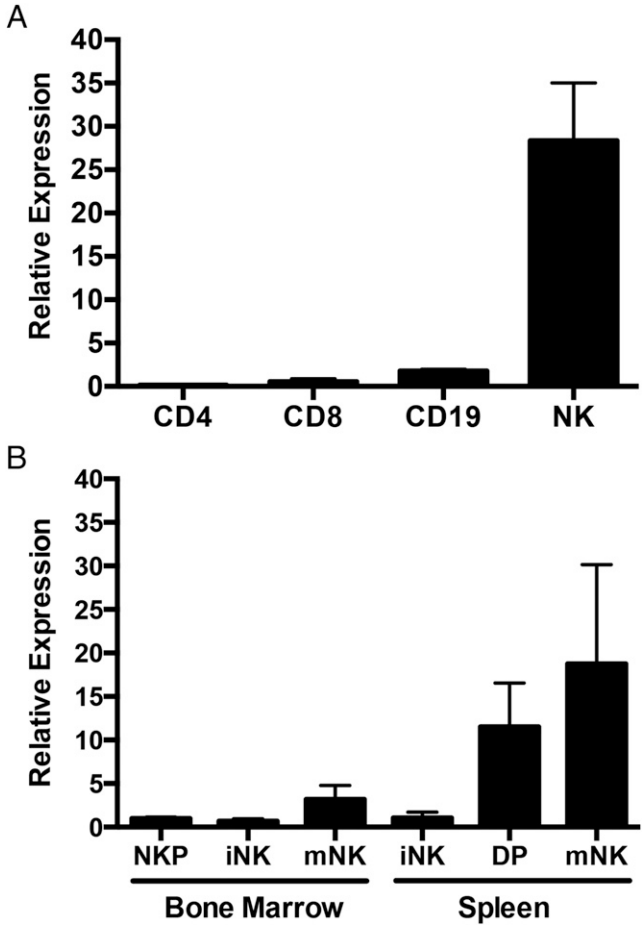

FIGURE 1. KLF12 is preferentially expressed in mature mouse NK cells. Quantitative PCR of *Klf12* expression in (**A**) sorted splenic populations defined as CD4$^+$ T cells: TCRβ$^+$NK1.1$^-$CD8$^-$CD4$^+$CD25$^-$; CD8$^+$ T cells: TCRβ$^+$NK1.1$^-$CD4$^-$CD8$^+$CD25$^-$; CD19$^+$ B cells: TCRβ$^-$NK1.1$^-$CD19$^+$; and NK cells: TCRβ$^-$NK1.1$^+$, and (**B**) sorted NK cell developmental stages in BM defined as NKP: CD3$^-$CD8$^-$CD19$^-$Ter119$^-$Gr1$^-$NK1.1$^-$DX5$^-$CD122$^+$, iNK: CD122$^+$NK1.1$^+$DX5$^-$, mNK: CD122$^+$NK1.1$^+$DX5$^+$. Developmental stages in spleen defined as iNK: TCRβ$^-$NK1.1$^+$CD27$^+$CD11b$^-$, DP: TCRβ$^-$NK1.1$^+$CD27$^+$CD11b$^+$, mNK: TCRβ$^-$NK1.1$^+$CD27$^-$CD11b$^+$. Data are representative of two experiments (n = 3 mice per experiment).

Abs and flow cytometry

Single-cell suspensions were incubated with anti-CD16 plus CD32 (2.4G2) mAb to block Fc receptors 15 min on ice and then stained with mAbs to cell surface or intracytoplasmic Ags of interest. mAbs were purchased from BD Biosciences, BioLegend, eBioscience, and Tonbo Biosciences. Samples were acquired on an LSR II or LSR Fortessa (BD Biosciences) and analyzed on FlowJo software (Tree Star).

Statistical analysis

The unpaired, two-tailed Student *t* test was used to analyze results in Prism GraphPad. A p value ≤ 0.05 was considered significant. Error bars represent SD.

Results

Klf12 is preferentially expressed in mature mouse NK cells

ImmGen results revealed that mouse NK cells preferentially expressed a novel transcription factor, KLF12. Consistent with ImmGen data, quantitative PCR from highly purified lymphocyte populations from splenocytes of C57BL/6 mice confirmed that NK cells expressed 25-fold more *Klf12* transcripts than $CD4^+$, $CD8^+$ T cells, and $CD19^+$ B cells (Fig. 1A). *Klf12* expression increased as splenic NK cells transitioned from semimature $CD27^+CD11b^+$ double positive (DP) to fully mature $CD27^-CD11b^+$ NK cells (Fig. 1B). Analysis of microarray and RNA sequencing (RNA-Seq) data from ImmGen indicated absence or low transcription of *Klf12* in all other hematopoietic cell types, including macrophages, monocytes, dendritic cells, granulocytes, mast cells, innate lymphoid cell (ILC)2, ILC3, γδ T cells, thymocytes, invariant NKT cells, hematopoietic stem cells, and virus-activated $CD8^+$ T cells (https://www.immgen.org). Furthermore, ILC1 do not express *Klf12* (33). Taken together, mouse NK cells preferentially express *Klf12*.

NK cell development and function are normal in KLF12-deficient mice

To investigate the role of KLF12 in NK cells, we generated *Klf12* knockout mice using a targeted vector to excise exon 3 of *Klf12* (Fig. 2A). Integration of the targeting vector was confirmed by the presence of a 6.44-kb band in the Southern blot of selected stem cell clones and a 5.7-kb band detected in mice by long range PCR (Fig. 2B, 2C). The *lacZ* and neomycin cassettes were removed by crossing to *Rosa26-Flippase* mice, resulting in progeny mice bearing loxP sites flanking exon 3 of *Klf12* (Fig. 2A). β-Actin Cre recombinase excised exon 3 of *Klf12* and the progeny were genotyped by PCR (Fig. 2D). *Klf12* transcripts without exon 3 were detected in whole splenocytes from $Klf12^{F/F}$ mice (Fig. 2E) that resulted in a premature translational stop codon (Fig. 2F). The putative truncated protein encodes a 65 aa peptide lacking all functional KLF12 protein domains. However, as none of the Abs currently available are KLF12 specific, we were unable to measure KLF12 protein in WT or knockout mice. The *Klf12*-null mice bred in predicted Mendelian ratios, and there were no abnormalities observed in growth or weight compared with WT or heterozygous littermates. T cell development in the thymus and spleen and T cell development in BM, spleen, lymph nodes, and the peritoneal cavity are normal in KLF12-deficient mice when compared with WT and heterozygous littermates (Supplemental Fig. 1). Additionally, stimulation of $CD4^+$ and $CD8^+$ T and B cells isolated from lymph nodes through their Ag receptors by immobilized anti-CD3 or anti-IgM, respectively, resulted in downstream signaling of ERK (Supplemental Fig. 2) and proliferation (Supplemental Fig. 3) equivalent to WT or heterozygous littermates.

Phenotypic analysis of $Klf12^{+/+}$, $Klf12^{F/+}$, and $Klf12^{F/F}$ NK cells was performed to determine whether KLF12 is required for NK cell development. We examined NK developmental subsets as defined by expression of CD27 and CD11b and expression of Ly49 and NKG2 activating and inhibitory receptors in the BM and spleen. $Klf12^{F/+}$ and $Klf12^{F/F}$ mice had normal frequencies and numbers of all NK cell developmental subsets in the BM and spleen, equivalent to $Klf12^{+/+}$ littermate controls. Expression of activating and inhibitory receptors was also similar to $Klf12^{+/+}$

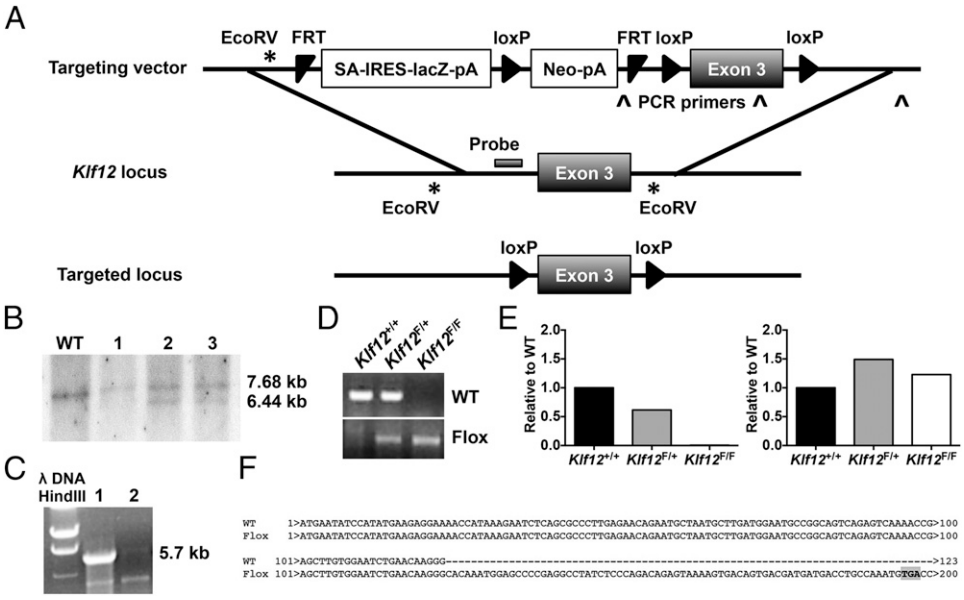

FIGURE 2. Targeted disruption of the *Klf12* locus. (**A**) Schematic of the targeting strategy into the *Klf12* locus to generate *Klf12* conditional knockout mice after excision of the *lacZ* and neo*mycin* cassettes by Flippase recombination. (**B**) Southern blot of gDNA from selected ES cell clones digested with EcoRV and hybridized to a probe indicated in (A). The 7.68-kb band is the WT allele and the 6.44-kb band is the targeted allele. (**C**) Long range PCR of gDNA from heterozygous (lane 1) and WT (lane 2) mice amplifying the 3′ arm of the targeting vector with primers indicated in (A). The 5.7 kb band is the targeted allele. (**D**) PCR of mouse gDNA from indicated genotypes. (**E**) Quantitative PCR amplifying exons 2–3 (left) or exons 5–6 (right) of *Klf12*. (**F**) PCR sequence of *Klf12* cDNA from WT or $Klf12^{F/F}$ β-actin Cre^+ mice. The premature stop codon is highlighted in gray. (E and F) Data are representative of $n = 3$ mice per genotype.

controls (Fig. 3A). Furthermore, the number and frequency of liver ILC1 and NK cells was equivalent in *Klf12*$^{+/+}$ and *Klf12*$^{F/F}$ mice (data not shown). Therefore, KLF12 deficiency does not affect NK cell development or expression of NK receptors.

We assessed whether KLF12 deficiency affected NK cell effector functions. *Klf12*$^{F/+}$ and *Klf12*$^{F/F}$ NK cells produced IFN-γ and degranulated similar to *Klf12*$^{+/+}$ NK cells upon stimulation with IL-12 and -18, anti-NK1.1, or PMA and ionomycin (Fig. 3B). Furthermore, the in vitro proliferative capacity of *Klf12*$^{F/+}$ and *Klf12*$^{F/F}$ NK cells upon stimulation with IL-15, the RMA lymphoma cell line, and MCMV m157 (ligand of the activating Ly49H receptor)–transduced RMA cells was comparable to *Klf12*$^{+/+}$ NK cells (Fig. 3C). Therefore, KLF12 deficiency does not affect the in vitro NK cell effector functions and cytokine- and Ag-driven proliferation in the knockout mice.

We also tested in vivo NK cell responses upon MCMV infection. *Klf12*$^{+/+}$, *Klf12*$^{F/+}$, and *Klf12*$^{F/F}$ mice were infected with Smith strain MCMV, and expansion of Ly49H$^+$ NK cells and viral titers were monitored over 28 d. Naive, uninfected *Klf12*$^{+/+}$, and *Klf12*$^{F/F}$ mice had a similar percentage of Ly49H$^+$ NK cells in the blood. After MCMV infection, there was comparable expansion of Ly49H$^+$ NK cells in *Klf12*$^{+/+}$, *Klf12*$^{F/+}$, and *Klf12*$^{F/F}$ mice. Viral titers in the blood and oral lavage were indistinguishable (Fig. 3D). Therefore, KLF12 deficiency does not alter NK cell effector functions in vitro and upon in vivo MCMV challenge.

KLF12-deficient NK cells intrinsically express more Btg3 transcripts

We hypothesized that redundancy or compensatory mechanisms with other KLF members may mask the effects of KLF12 deficiency in NK cell development and function. Therefore, we performed RNA-Seq to determine the effects of KLF12 deficiency on the transcriptome of *Klf12*$^{F/F}$ mice. Total RNA was collected from purified T cells, B cells, and NK cells from 6-wk-old *Klf12*$^{+/+}$ and *Klf12*$^{F/F}$ β-actin Cre$^-$ littermate male mice. *Klf12*$^{F/F}$ NK cells had increased transcripts involved in regulating cellular transcription, NF-κB activity, and cellular division compared with *Klf12*$^{+/+}$ NK cells (Fig. 4A). Of the differentially expressed genes, we confirmed increased expression of B cell translocation gene 3, *Btg3*, encoding an antiproliferative protein, in *Klf12*$^{F/F}$ NK cells but not in *Klf12*$^{F/F}$ T cells, B cells, or *Klf12*$^{+/+}$ NK cells (Fig. 4B). Furthermore, *Klf12*$^{F/F}$ NK cells isolated from mixed BM chimeric mice had more *Btg3* transcripts than *Klf12*$^{+/+}$ NK cells purified from the same mice (Fig. 4C). Altogether, KLF12-deficient NK cells intrinsically express more *Btg3* transcripts. By contrast, no significant transcriptional differences were observed comparing

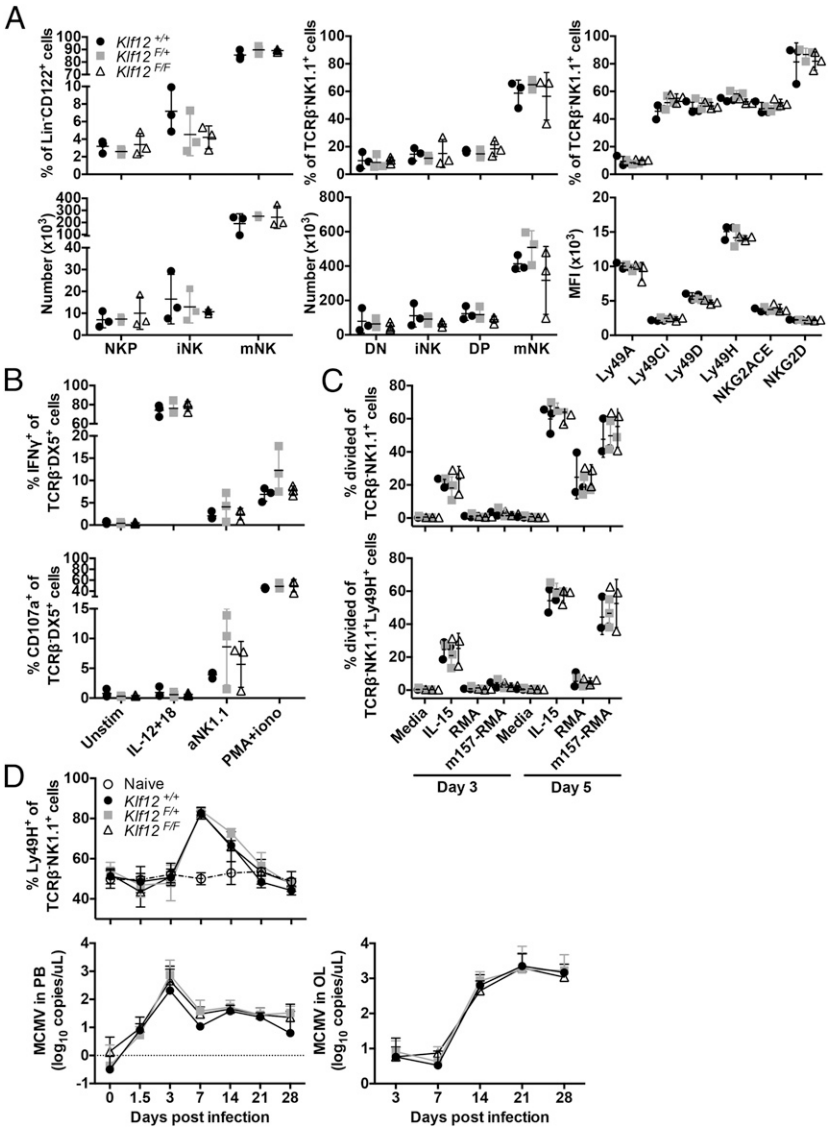

FIGURE 3. NK cell development and function are normal in KLF12-deficient mice. (**A**) Percentage and total cell numbers of BM (left panels) and splenic (middle panels) NK cell developmental subsets in *Klf12*$^{+/+}$ (circle), *Klf12*$^{F/+}$ (square), and *Klf12*$^{F/F}$ (triangle) mice. Double negative (DN) NK cell developmental subset defined as TCRβ$^-$NK1.1$^+$CD27$^-$CD11b$^-$. NK receptor expression (right panels) gated on splenic TCRβ$^-$NK1.1$^+$ NK cells. (**B**) IFN-γ and CD107a staining gated on TCRβ$^-$DX5$^+$ NK cells after in vitro stimulation for 6 h. (A and B) Data are representative of three experiments (n = 3 mice per genotype per experiment). (**C**) Proliferation of TCRβ$^-$NK1.1$^+$ and TCRβ$^-$NK1.1$^+$Ly49H$^+$ NK cells after in vitro stimulation. Data are representative of two experiments (n = 3 mice per genotype per experiment). (**D**) Percentage of Ly49H$^+$ cells gated on TCRβ$^-$NK1.1$^+$ NK cells in the blood and viral titers in the blood and oral lavage following MCMV infection. Data are representative of two experiments (n = 2–4 mice per genotype per experiment).

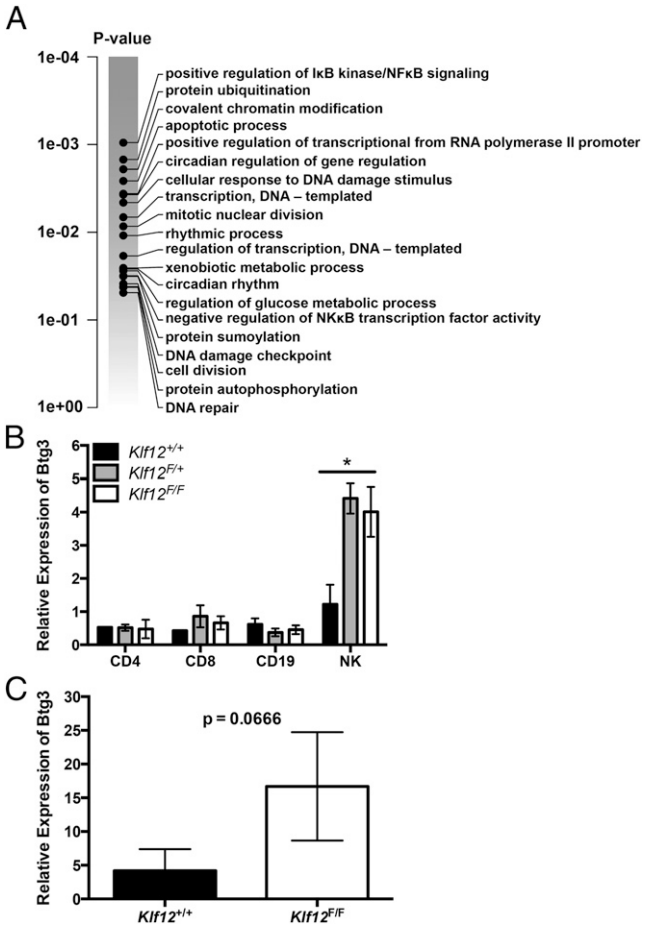

FIGURE 4. KLF12-deficient NK cells intrinsically express more *Btg3* transcripts. (**A**) Gene set enrichment analysis of $Klf12^{+/+}$ and $Klf12^{F/F}$ splenic NK cells defined as $CD3^-NK1.1^+$ (n = 3 mice per genotype). Quantitative PCR of *Btg3* expression in (**B**) sorted splenic populations defined as $CD4^+$ T cells: $TCR\beta^+NK1.1^-CD8^-CD4^+CD25^-$; $CD8^+$ T cells: $TCR\beta^+NK1.1^-CD4^-CD8^+CD25^-$; $CD19^+$ B cells: $CD3^-NK1.1^-CD19^+$; NK cells: $CD3^-NK1.1^+$, and (**C**) sorted splenic $TCR\beta^-NK1.1^+$ NK cells from $Klf12^{+/+}$ and $Klf12^{F/F}$ BM chimeric mice. (B and C) Data are representative of two experiments [n = 2–3 mice per genotype per experiment for (B) and n = 3 mice per experiment for (C)]. Full transcription datasets are available at gene expression omnibus GSE128962.

$Klf12^{+/+}$ and $Klf12^{F/F}$ T cells and B cells, indicating that the alterations in $Klf12^{F/F}$ NK cells were cell intrinsic.

KLF12-deficient NK cells are competitively disadvantaged

Although in the intact KLF12-deficient mice we observed no marked alteration in NK cell phenotype, in many cases gene deficiencies in knockout mice are only revealed when the gene-deficient cells are in competition with WT cells. Therefore, we generated mixed BM chimeras of $Klf12^{+/+}$ and $Klf12^{F/F}$ cells at a 1:1 ratio to assess the role of KLF12 in NK cells in a competitive setting. After reconstitution of the hematopoietic cells for about 2 mo, we observed reduced absolute numbers of $Klf12^{F/F}$ NK cell developmental subsets in the BM and spleen (Fig. 5A). The levels of expression (as reflected by mean fluorescence intensity [MFI]) of activating and inhibitory NK receptors were comparable between $Klf12^{+/+}$ and $Klf12^{F/F}$ cells (Fig. 5A). In a competitive setting, $Klf12^{F/F}$ NK cells produced less IFN-γ upon IL-12 plus IL-18 stimulation but more IFN-γ upon anti-NK1.1 stimulation. $Klf12^{F/F}$ NK cells also degranulated more than $Klf12^{+/+}$ NK cells upon anti-NK1.1 stimulation (Fig. 5B). Thus, KLF12 deficiency alters NK cell development and effector function, but not receptor expression, when the NK cells are developed in a competitive setting. By contrast, $Klf12^{F/F}$ and WT $CD4^+$ and $CD8^+$ T cells responded equivalently to MCMV infection (Supplemental Fig. 4).

Because we observed increased expression of the anti-proliferative gene, *Btg3*, in $Klf12^{F/F}$ NK cells, we directly assessed whether in vitro proliferation of $Klf12^{F/F}$ NK cells was preferentially affected in BM chimeras compared with $Klf12^{+/+}$ NK cells. We observed a statistically significant proliferative impairment of $Klf12^{F/F}$ NK cells in BM chimeric mice in response to IL-15 or coculture with m157-expressing RMA lymphoma cells compared with $Klf12^{+/+}$ NK cells (Fig. 5C). $Klf12^{F/F}$ NK cells also had impaired proliferation in vivo when BM chimeric mice were infected with MCMV. At day 7 after MCMV infection, we observed a statistically significant reduction in the numbers of $Ly49H^+$ $Klf12^{F/F}$ NK cells compared with $Ly49H^+$ $Klf12^{+/+}$ NK cells (Fig. 5D). Furthermore, this observation was recapitulated when a mixture of mature $Ly49H^+$ $Klf12^{+/+}$ and $Klf12^{F/F}$ NK cells were adoptively transferred into Ly49H-deficient mice and infected with MCMV (Fig. 5E). Together, these findings reveal that KLF12 deficiency impairs NK cells to proliferate in response to cytokines and Ags when in competition with WT NK cells.

KLF12-deficient NK cells from BM chimeric mice have altered common γ-chain receptor expression but normal IL-15R signaling

The common γ-chain (CD132) cytokine receptor family is important for lymphocyte development during BM reconstitution and for lymphocyte activation. We observed slightly decreased CD132 expression on $Klf12^{F/F}$ NK cells compared with $Klf12^{+/+}$ NK cells in BM chimeric mice, whereas expression of the β-chain (CD122) was identical. Furthermore, CD132 expression was significantly decreased on all $Klf12^{F/F}$ splenic NK cell developmental subsets compared with $Klf12^{+/+}$ NK cells (Fig. 6A). Expression of CD132, but not CD122, was decreased on KLF12-deficient NK cells from mixed BM chimeric mice.

We examined which members of the common γ-chain cytokine receptor family might be affected by the decreased expression of CD132 on KLF12-deficient NK cells. We hypothesized that the responsiveness of IL-15 might be affected by KLF12 deficiency because it is important for NK cell development (34, 35). We examined the phosphorylation of STAT5 in NK cells from BM chimeric mice upon IL-15 stimulation as a functional measure of responsiveness to IL-15. The percentages of NK cells responding and MFI of p-STAT5 were similar between $Klf12^{+/+}$ and $Klf12^{F/F}$ NK cells upon culture with low and high concentrations of IL-15. Thus, responsiveness to IL-15 remains intact and unaffected by KLF12 deficiency.

KLF12-deficient NK cells from BM chimeric mice have increased IL-21R expression and signaling correlating with less NK cell proliferation

The IL-21R is another member of the common γ-chain cytokine receptor family that has been implicated in NK cell maturation and proliferation (36–38). Although IL-21R is dispensable for mouse NK cell development, IL-21 induces their maturation but inhibits their proliferation (37). Furthermore, IL-21 enhances NK cell responses against tumors expressing ligands for the activating NK receptor, NKG2D (39). Given the inhibitory role of the IL-21R in NK cell proliferation, we assessed IL-21R expression on NK cells in BM chimeric mice. Interestingly, we observed higher levels of IL-21R expression on splenic $Klf12^{F/F}$ NK cells. This was also evident on all splenic $Klf12^{F/F}$ NK cell developmental subsets. In fact, the most immature subset of NK cells, lacking

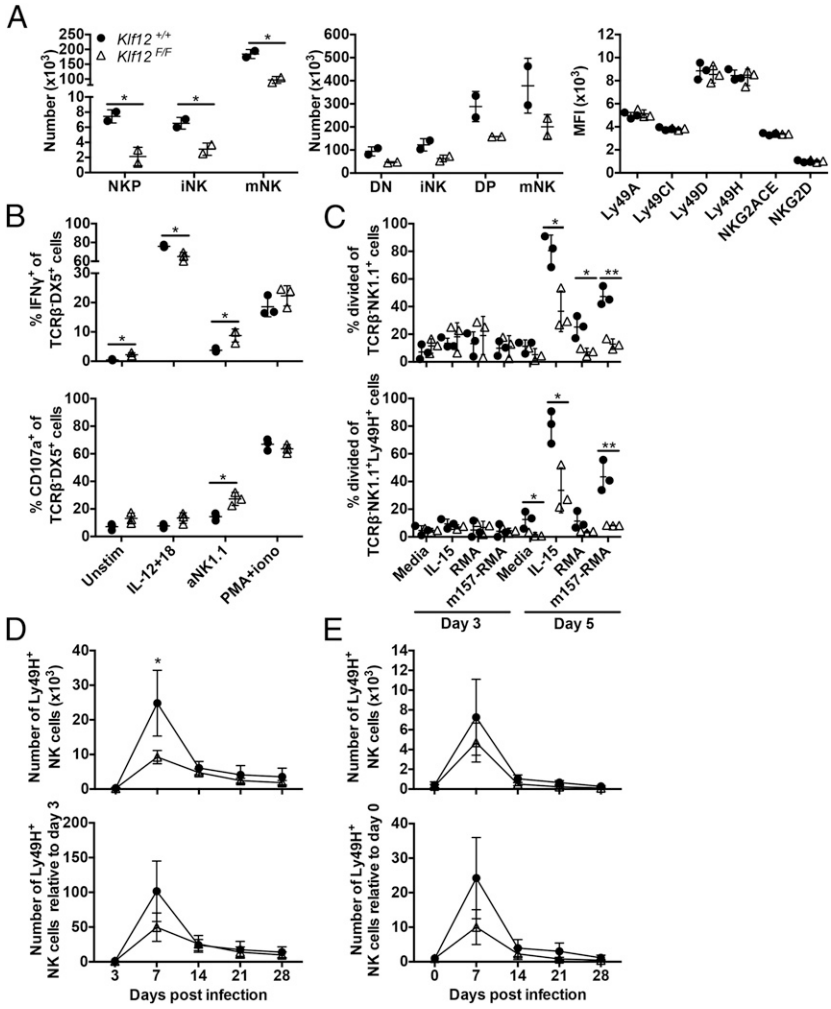

FIGURE 5. KLF12-deficient NK cells are competitively disadvantaged. (**A**) Total cell numbers of BM (left panel) and splenic (middle panel) NK cell subsets in BM chimeras at a 1:1 ratio of *Klf12*$^{+/+}$ (circle) and *Klf12*$^{F/F}$ (triangle) cells. NK receptor expression (right panel) gated on splenic TCRβ$^-$NK1.1$^+$ NK cells. Data are representative of six experiments (n = 3 mice per experiment). (**B**) IFN-γ and CD107a staining gated on TCRβ$^-$DX5$^+$ NK cells after in vitro stimulation for 6 h. Data are representative of three experiments (n = 3 mice per experiment). (**C**) Proliferation of TCRβ$^-$NK1.1$^+$ and TCRβ$^-$NK1.1$^+$Ly49H$^+$ NK cells after in vitro stimulation. Data are representative of eight experiments (n = 2–3 mice/experiment). (**D** and **E**) Number (top panels) and relative change in number (bottom panels) of TCRβ$^-$NK1.1$^+$Ly49H$^+$ NK cells in the blood during MCMV infection in (D) BM chimeras and (E) adoptive transfer model where a 1:1 ratio of *Klf12*$^{+/+}$ and *Klf12*$^{F/F}$ TCRβ$^-$NK1.1$^+$Ly49H$^+$ NK cells were transferred into Ly49H-deficient hosts 1 d prior to MCMV infection. Data are representative of (D) three experiments (n = 3–6 mice per experiment) or (E) six experiments (n = 3–5 mice per experiment). $^*p < 0.05$, $^{**}p < 0.005$.

expression of CD27 and CD11b (termed double negative [DN]), expressed the highest levels of the IL-21R (Fig. 7A). Thus, expression of the IL-21R is increased on mouse NK cells by KLF12 deficiency.

We measured p-STAT3 expression upon IL-21 stimulation to determine whether increased IL-21R expression on KLF12-deficient NK cells resulted in increased IL-21–induced signaling. At a low concentration of IL-21, we detected increased percentages and levels of expression (MFI) of p-STAT3 in *Klf12*$^{F/F}$ NK cells compared with *Klf12*$^{+/+}$ NK cells in the mixed BM chimeras (Fig. 7B). Furthermore, it was the most immature subset of NK cells (DN) that upregulated p-STAT3 the most compared with other developmental subsets. This is not surprising because the DN subset expressed the highest levels of IL-21R and therefore should have increased p-STAT3 upregulation.

Subsequently, we evaluated whether increased IL-21R expression and signaling in KLF12-deficient NK cells correlated with greater IL-21–mediated inhibition of proliferation. We cultured splenocytes from mixed BM chimeric mice with IL-15 in the presence or absence of IL-21 and monitored the maturation and percentage of NK cells for 7 d. We observed reduced percentages of *Klf12*$^{F/F}$ NK cells upon IL-15 culture compared with *Klf12*$^{+/+}$ NK cells (Fig. 7C). By day 7 of IL-15 culture, all NK cells had proliferated (measured by the percentage of divided cells), and we were unable to observe differences in proliferation as we observed on day 5 of IL-15 culture (Fig. 5C). Addition of IL-21 to the culture reduced the overall percentages of NK cells and inhibited the proliferation of *Klf12*$^{F/F}$ NK cells more than *Klf12*$^{+/+}$ NK cells. In fact, the most immature *Klf12*$^{F/F}$ NK cell DN subset was significantly reduced in percentage by IL-21, but there was no difference in proliferation of total NK cells, possibly because the *Klf12*$^{F/F}$ NK cell DN subset was driven to mature in response to the IL-21. Although there was a higher percentage of *Klf12*$^{F/F}$ semimature CD27$^+$CD11b$^+$ DP subset of NK cells, they did not proliferate as well as their *Klf12*$^{+/+}$ counterparts. KLF12 deficiency in NK cells resulted in increased expression and signaling of the IL-21R. This enhanced IL-21R signaling correlated with greater inhibition of NK cell proliferation, particularly in the most immature DN NK cell subset.

IL-21 stimulation induces Btg3 expression in NK cells

Given that KLF12-deficient NK cells have impaired proliferation, intrinsically express more *Btg3* transcripts, and express higher levels of the IL-21R, we sought to determine whether IL-21 might inhibit NK cell proliferation via BTG3. To address this, we cultured enriched WT NK cells in IL-21 and assessed *Btg3* expression. We observed a significant increase in *Btg3* expression after 2 h of IL-21 stimulation and then a progressive decrease in expression with time. Even after 24 h of continual IL-21 stimulation, *Btg3* expression remains significantly increased (Fig. 8). Thus, IL-21 directly induces *Btg3* expression in NK cells and correlates with the decreased proliferative activity.

Discussion

Unlike their other lymphocyte counterparts, NK cells have the unique ability to recognize and lyse target cells without prior

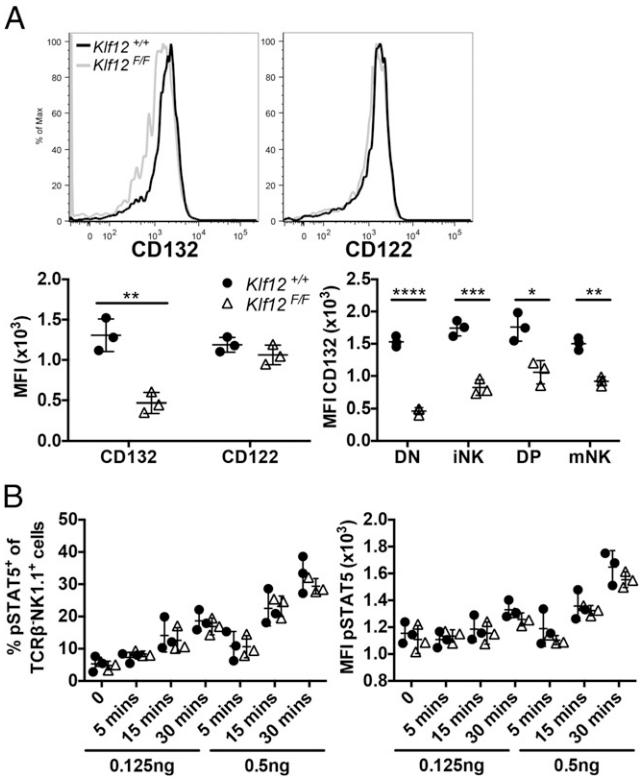

FIGURE 6. KLF12-deficient NK cells from BM chimeric mice have decreased CD132 expression but normal responsiveness to IL-15. (**A**) Representative histogram of CD132 and CD122 expression on *Klf12*$^{+/+}$ (black line) and *Klf12*$^{F/F}$ (gray line) splenic TCRβ$^-$NK1.1$^+$ NK cells. MFI of CD132 and CD122 expression on splenic TCRβ$^-$NK1.1$^+$ NK cells (left panel) and NK cell developmental subsets (right panel). Data are representative of two experiments (n = 3 mice per experiment). (**B**) Percentage and MFI of p-STAT5 in splenic TCRβ$^-$NK1.1$^+$ NK cells upon ex vivo IL-15 stimulation. Data are representative of five experiments (n = 2–3 mice per experiment). $^*p < 0.05$, $^{**}p < 0.005$, $^{***}p < 0.001$, $^{****}p < 0.0001$.

exposure via expression of their germline-encoded receptors. However, there are no NK cell-specific genes that are exclusively expressed by all NK cells. Transcription factors, signaling components downstream of NK activating or inhibitory receptors, and even expression of certain NK activating receptors are shared among NK cells and other lymphocytes. From the ImmGen studies, we identified *Klf12*, encoding a novel transcription factor, to be preferentially expressed in mouse NK cells and not in ILC1, ILC2, ILC3, T cells, or B cells. In this study, we generated *Klf12* knockout mice to assess its role in NK cell development or effector function. We used β-actin Cre recombinase to delete KLF12 in all cells. We observed normal lymphocyte development, proliferation, and activation in KLF12-deficient mice (Supplemental Figs. 1–4). We also generated mice in which KLF12 was conditionally deleted only in NK cells using *Ncr1-Cre* mice with similar results (data not shown). However, we found that in competitive mixed BM chimeras, KLF12-deficient NK cells demonstrated less robust proliferation that correlated with higher levels of expression of *Btg3*, an antiproliferative gene, which is upregulated by IL-21. Notably, KLF12-deficient NK cells express higher levels of IL-21R and have elevated p-STAT3 signaling in response to IL-21 compared with WT NK cells.

In the absence of competition with WT NK cells, KLF12 is dispensable for NK cell lineage commitment, development, and effector functions. KLF12-deficient NK cells produced IFN-γ and degranulated equivalently as WT NK cells. Furthermore, NK cell proliferation in vitro and in vivo in the context of MCMV infection

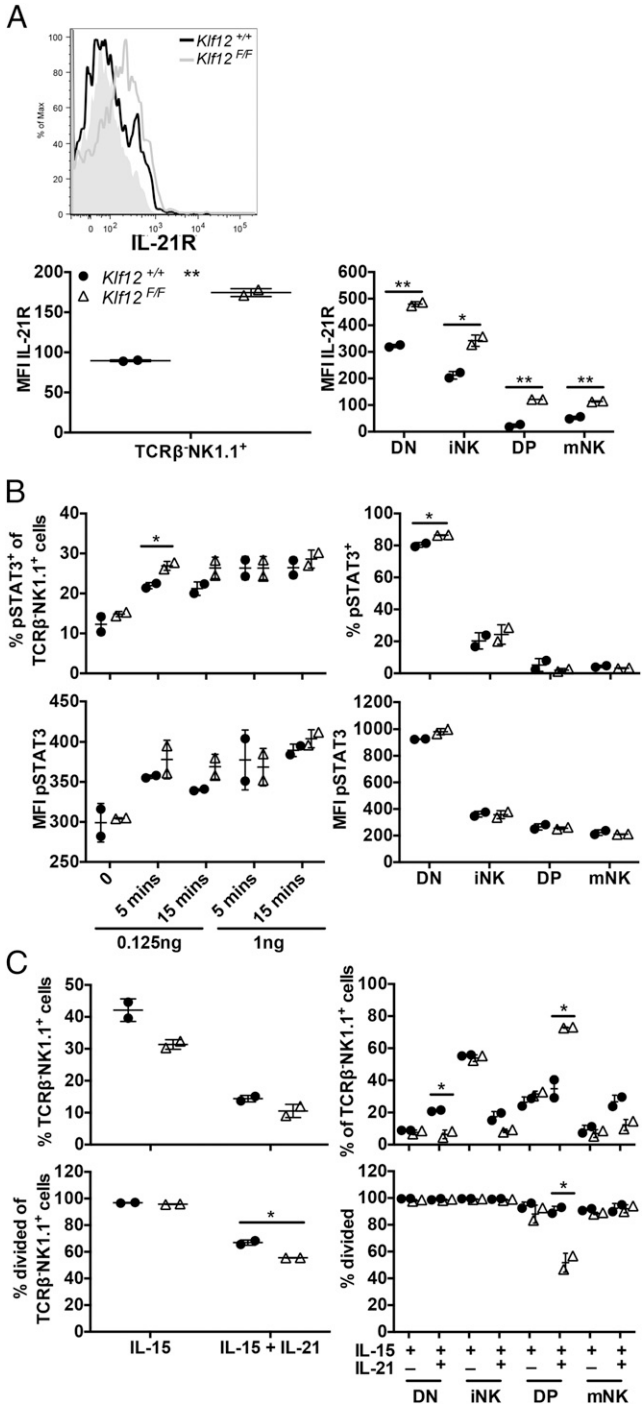

FIGURE 7. IL-21R expression and signaling are increased in KLF12-deficient NK cells from mixed BM chimeric mice. (**A**) Representative histogram of IL-21R expression on *Klf12*$^{+/+}$ (black line) and *Klf12*$^{F/F}$ (gray line) splenic TCRβ$^-$NK1.1$^+$ NK cells. The gray-filled histogram is the fluorescence minus one control. MFI of IL-21R expression on splenic TCRβ$^-$NK1.1$^+$ NK cells (left panel) and NK cell developmental subsets (right panel). Data are representative of two experiments (n = 2 mice per experiment). (**B**) Percentage and MFI of p-STAT3 in splenic TCRβ$^-$NK1.1$^+$ NK cells (left panels) upon IL-21 stimulation ex vivo and NK cell developmental subsets (right panels) upon 0.125 ng/ml IL-21 stimulation ex vivo for 15 min. Data are representative of two experiments (n = 2 mice per experiment). (**C**) Percentage of splenic TCRβ$^-$NK1.1$^+$ NK cells (left panels) and NK cell developmental subsets (right panels) after 7 d of in vitro culture in 10 ng/ml IL-15 in the absence or presence of 100 ng/ml IL-21. Data are representative of two experiments (n = 2 mice per experiment). $^*p < 0.05$, $^{**}p < 0.005$.

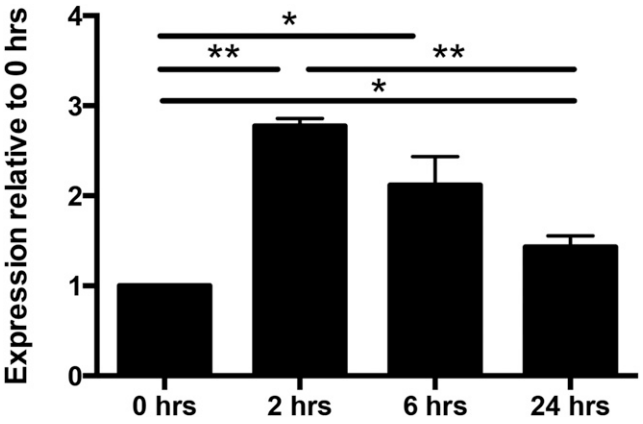

FIGURE 8. IL-21 induced *Btg3* expression in NK cells. Quantitative PCR of *Btg3* expression in enriched C57BL/6 WT splenic TCRβ$^-$NK1.1$^+$ NK cells cultured with 100 ng/ml of IL-21 for the indicated times. Expression of *Btg3* was normalized to 0 h. Data are representative of three experiments (n = 2–3 mice per experiment). *$p < 0.05$, **$p < 0.005$.

was also unperturbed by KLF12 deficiency in the *Klf12*$^{F/F}$ mice. The lack of a NK cell phenotype may be due to compensatory mechanisms or redundancy among other members of the KLF family, particularly KLF3 and KLF8. Both KLF3 and KLF8 share the conserved PVDLS domain with KLF12 (14, 16), and KLF3 is highly expressed in mouse NK cells (https://www.immgen.org/). Interestingly, KLF12-deficient NK cells have similar expression of KLF3 and KLF3 transcripts as WT NK cells (data not shown, GSE128962). However, we were unable to address whether compensatory mechanisms masked KLF12 deficiency in vivo because of embryonic lethality in C57BL/6 KLF3-deficient mice and KLF3 and KLF8–double knockout mice (Ref. 40 and personal communication with M. Crossley). Further studies generating NK cell-specific double or triple knockout mice would be required to uncover potential compensatory pathways in KLF12-deficient NK cells.

Recent studies have shown that KLF12 regulates proliferation of many cancer cell lines. Overexpression of KLF12 in endometrial and lung cancer cell lines correlated with decreased apoptosis, increased cellular proliferation, and increased in vivo tumor growth (41–43). Conversely, downregulation of KLF12 resulted in a proliferative defect in multiple cancer cell lines (19, 23, 44–47). These observations were recapitulated in primary human cancer cells and mouse kidney cells (48, 49). In this study, we observed a proliferative defect in KLF12-deficient NK cells in a competitive setting in BM chimeric mice upon Ag- and cytokine-mediated proliferation. Although we observed a proliferative impairment upon IL-15 stimulation, the expression of p-STAT5 was comparable between KLF12-deficient and WT NK cells. Interestingly, we detected increased p-STAT3 expression in KLF12-deficient NK cells upon IL-21 stimulation, which correlated with greater IL-21–mediated inhibition of proliferation. Similarly, overexpression of KLF12 in an endometrial adenocarcinoma cell line resulted in decreased p-STAT3 expression upon LIF stimulation, which inhibits cellular differentiation (42). The proliferative defect in KLF12-deficient NK cells might be an intrinsic effect of p-STAT3 expression.

Alternatively, the proliferative impairment observed in KLF12-deficient NK cells may be due to the increased expression of an antiproliferative transcription factor, *Btg3*. BTG3 is a member of the antiproliferative BTG/Tob protein family that inhibits entry into the S-phase of cell cycle progression. It has been shown that upon DNA damage, p53 binds to the *BTG3* promoter and induces its expression to regulate cell cycle checkpoints (50). Downregulation of BTG3 expression is associated with enhanced cell proliferation, growth, and migration (51, 52). Conversely, overexpression of BTG3 is associated with suppressed proliferation, reduced cancer invasiveness, and cellular apoptosis in primary cancers and cancer cell lines (53–55).

During MCMV infection, IL-21 induces mouse NK cells to produce IL-10, which affects dendritic cell activation and CD8$^+$ T cell responses (38, 56–58). We also observed proliferative impairment of KLF12-deficient NK cells during MCMV infection in the mixed BM chimeric mice and in the adoptive transfer of mature NK cells. IL-21 present during MCMV infection may be inhibiting NK cell proliferation and inducing IL-10 production to modulate adaptive immune responses. However, we observed comparable numbers of KLF12-deficient and WT CD4$^+$ AND CD8$^+$ naive, effector memory, and MCMV-specific NKG2D$^+$ CD8$^+$ T cells in MCMV-infected BM chimeric mice (Supplemental Fig. 4), suggesting that the T cell responses against MCMV are normal.

Although the IL-21R is not required for mouse NK cell development, IL-21 induces NK cell maturation, inhibits their proliferation, and enhances their NKG2D-mediated antitumor response (36–39). In this study, we noted increased expression of the IL-21R on KLF12-deficient NK cells compared with WT NK cells in mixed BM chimeric mice. Increased IL-21R expression resulted in enhanced IL-21 signaling and correlated with inhibition of KLF12-deficient NK cell proliferation. It appears as though IL-21 is driving NK cell maturation, but in the absence of KLF12 NK cell maturation may be arrested at the semimature DP stage. This is consistent with the fact that KLF12 is upregulated at the semimature DP stage. Moreover, IL-21 alone induces *Btg3* expression in NK cells, which may reinforce the proliferative defect in KLF12-deficient NK cells in competitive situations. Conditional deletion of *Btg3* and *Il21r* in NK cells will be needed to definitively address this hypothesis.

Acknowledgments

We thank the UCSF Cell and Genome Engineering Core for assistance and Dr. Hong-Erh Liang in the Dr. Richard Locksley laboratory for guidance in generating *Klf12* conditional knockout mice, the ImmGen Consortium for performing the RNA-Seq experiment, Dr. Alice Chan in the Dr. Mark Anderson laboratory for technical guidance, and members of the Lanier Lab for helpful discussions.

Disclosures

The authors have no financial conflicts of interest.

References

1. Biron, C. A., K. S. Byron, and J. L. Sullivan. 1989. Severe herpesvirus infections in an adolescent without natural killer cells. *N. Engl. J. Med.* 320: 1731–1735.
2. Mace, E. M., and J. S. Orange. 2019. Emerging insights into human health and NK cell biology from the study of NK cell deficiencies. *Immunol. Rev.* 287: 202–225.
3. Mace, E. M., A. P. Hsu, L. Monaco-Shawver, G. Makedonas, J. B. Rosen, L. Dropulic, J. I. Cohen, E. P. Frenkel, J. C. Bagwell, J. L. Sullivan, et al. 2013. Mutations in GATA2 cause human NK cell deficiency with specific loss of the CD56(bright) subset. *Blood* 121: 2669–2677.
4. Notarangelo, L. D., and E. Mazzolari. 2006. Natural killer cell deficiencies and severe varicella infection. *J. Pediatr.* 148: 563–564, author reply 564.
5. Lam, V. C., and L. L. Lanier. 2017. NK cells in host responses to viral infections. *Curr. Opin. Immunol.* 44: 43–51.
6. Orange, J. S., and C. A. Biron. 1996. Characterization of early IL-12, IFN-alphabeta, and TNF effects on antiviral state and NK cell responses during murine cytomegalovirus infection. *J. Immunol.* 156: 4746–4756.
7. Orange, J. S., B. Wang, C. Terhorst, and C. A. Biron. 1995. Requirement for natural killer cell-produced interferon gamma in defense against murine cytomegalovirus infection and enhancement of this defense pathway by interleukin 12 administration. *J. Exp. Med.* 182: 1045–1056.
8. Orange, J. S., and C. A. Biron. 1996. An absolute and restricted requirement for IL-12 in natural killer cell IFN-gamma production and antiviral defense. Studies of natural killer and T cell responses in contrasting viral infections. *J. Immunol.* 156: 1138–1142.
9. Arase, H., E. S. Mocarski, A. E. Campbell, A. B. Hill, and L. L. Lanier. 2002. Direct recognition of cytomegalovirus by activating and inhibitory NK cell receptors. *Science* 296: 1323–1326.

10. Smith, H. R., J. W. Heusel, I. K. Mehta, S. Kim, B. G. Dorner, O. V. Naidenko, K. Iizuka, H. Furukawa, D. L. Beckman, J. T. Pingel, et al. 2002. Recognition of a virus-encoded ligand by a natural killer cell activation receptor. *Proc. Natl. Acad. Sci. USA* 99: 8826–8831.
11. Dokun, A. O., S. Kim, H. R. Smith, H. S. Kang, D. T. Chu, and W. M. Yokoyama. 2001. Specific and nonspecific NK cell activation during virus infection. *Nat. Immunol.* 2: 951–956.
12. Sun, J. C., J. N. Beilke, and L. L. Lanier. 2009. Adaptive immune features of natural killer cells. [Published erratum appears in 2009 *Nature* 457: 1168.] *Nature* 457: 557–561.
13. Min-Oo, G., and L. L. Lanier. 2014. Cytomegalovirus generates long-lived antigen-specific NK cells with diminished bystander activation to heterologous infection. *J. Exp. Med.* 211: 2669–2680.
14. Dang, D. T., J. Pevsner, and V. W. Yang. 2000. The biology of the mammalian Krüppel-like family of transcription factors. *Int. J. Biochem. Cell Biol.* 32: 1103–1121.
15. Roth, C., M. Schuierer, K. Günther, and R. Buettner. 2000. Genomic structure and DNA binding properties of the human zinc finger transcriptional repressor AP-2rep (KLF12). *Genomics* 63: 384–390.
16. Schuierer, M., K. Hilger-Eversheim, T. Dobner, A. K. Bosserhoff, M. Moser, J. Turner, M. Crossley, and R. Buettner. 2001. Induction of AP-2alpha expression by adenoviral infection involves inactivation of the AP-2rep transcriptional corepressor CtBP1. *J. Biol. Chem.* 276: 27944–27949.
17. Suda, S., T. Rai, E. Sohara, S. Sasaki, and S. Uchida. 2006. Postnatal expression of KLF12 in the inner medullary collecting ducts of kidney and its transactivation of UT-A1 urea transporter promoter. *Biochem. Biophys. Res. Commun.* 344: 246–252.
18. Shen, X., Y. Hu, Y. Jiang, H. Liu, L. Zhu, X. Jin, H. Shan, X. Zhen, L. Sun, G. Yan, and H. Sun. 2013. Krüppel-like factor 12 negatively regulates human endometrial stromal cell decidualization. *Biochem. Biophys. Res. Commun.* 433: 11–17.
19. Nakamura, Y., T. Migita, F. Hosoda, N. Okada, M. Gotoh, Y. Arai, M. Fukushima, M. Ohki, S. Miyata, K. Takeuchi, et al. 2009. Krüppel-like factor 12 plays a significant role in poorly differentiated gastric cancer progression. *Int. J. Cancer* 125: 1859–1867.
20. Imhof, A., M. Schuierer, O. Werner, M. Moser, C. Roth, R. Bauer, and R. Buettner. 1999. Transcriptional regulation of the AP-2alpha promoter by BTEB-1 and AP-2rep, a novel wt-1/egr-related zinc finger repressor. *Mol. Cell. Biol.* 19: 194–204.
21. Zhang, P., P. Basu, L. C. Redmond, P. E. Morris, J. W. Rupon, G. D. Ginder, and J. A. Lloyd. 2005. A functional screen for Krüppel-like factors that regulate the human gamma-globin gene through the CACCC promoter element. *Blood Cells Mol. Dis.* 35: 227–235.
22. Huang, C., Y. Jiang, J. Zhou, Q. Yan, R. Jiang, X. Cheng, J. Xing, L. Ding, J. Sun, G. Yan, and H. Sun. 2017. Increased Krüppel-like factor 12 in recurrent implantation failure impairs endometrial decidualization by repressing Nur77 expression. *Reprod. Biol. Endocrinol.* 15: 25.
23. Kim, S. H., Y. Y. Park, S. N. Cho, O. Margalit, D. Wang, and R. N. DuBois. 2016. Krüppel-like factor 12 promotes colorectal cancer growth through early growth response protein 1. *PLoS One* 11: e0159899.
24. Zhang, H., X. Zhu, J. Chen, Y. Jiang, Q. Zhang, C. Kong, J. Xing, L. Ding, Z. Diao, X. Zhen, et al. 2015. Krüppel-like factor 12 is a novel negative regulator of forkhead box O1 expression: a potential role in impaired decidualization. *Reprod. Biol. Endocrinol.* 13: 80.
25. Zhang, Q., H. Zhang, Y. Jiang, B. Xue, Z. Diao, L. Ding, X. Zhen, H. Sun, G. Yan, and Y. Hu. 2015. MicroRNA-181a is involved in the regulation of human endometrial stromal cell decidualization by inhibiting Krüppel-like factor 12. *Reprod. Biol. Endocrinol.* 13: 23.
26. Kamimura, Y., and L. L. Lanier. 2014. Rapid and sequential quantitation of salivary gland-associated mouse cytomegalovirus in oral lavage. *J. Virol. Methods* 205: 53–56.
27. Trapnell, C., A. Roberts, L. Goff, G. Pertea, D. Kim, D. R. Kelley, H. Pimentel, S. L. Salzberg, J. L. Rinn, and L. Pachter. 2012. Differential gene and transcript expression analysis of RNA-seq experiments with TopHat and Cufflinks. [Published erratum appears in 2012 *Nat. Protoc.* 9: 2513.] *Nat. Protoc.* 7: 562–578.
28. Kim, D., G. Pertea, C. Trapnell, H. Pimentel, R. Kelley, and S. L. Salzberg. 2013. TopHat2: accurate alignment of transcriptomes in the presence of insertions, deletions and gene fusions. *Genome Biol.* 14: R36.
29. Picelli, S., A. K. Björklund, O. R. Faridani, S. Sagasser, G. Winberg, and R. Sandberg. 2013. Smart-seq2 for sensitive full-length transcriptome profiling in single cells. *Nat. Methods* 10: 1096–1098.
30. Picelli, S., O. R. Faridani, A. K. Björklund, G. Winberg, S. Sagasser, and R. Sandberg. 2014. Full-length RNA-seq from single cells using Smart-seq2. *Nat. Protoc.* 9: 171–181.
31. Trombetta, J. J., D. Gennert, D. Lu, R. Satija, A. K. Shalek, and A. Regev. 2014. Preparation of single-cell RNA-seq libraries for next generation sequencing. *Curr. Protoc. Mol. Biol.* 107: 4.22.1–4.22.17.
32. Huang, W., B. T. Sherman, and R. A. Lempicki. 2009. Systematic and integrative analysis of large gene lists using DAVID bioinformatics resources. *Nat. Protoc.* 4: 44–57.
33. Seillet, C., N. D. Huntington, P. Gangatirkar, E. Axelsson, M. Minnich, H. J. Brady, M. Busslinger, M. J. Smyth, G. T. Belz, and S. Carotta. 2014. Differential requirement for Nfil3 during NK cell development. *J. Immunol.* 192: 2667–2676.
34. Kennedy, M. K., M. Glaccum, S. N. Brown, E. A. Butz, J. L. Viney, M. Embers, N. Matsuki, K. Charrier, L. Sedger, C. R. Willis, et al. 2000. Reversible defects in natural killer and memory CD8 T cell lineages in interleukin 15-deficient mice. *J. Exp. Med.* 191: 771–780.
35. Lodolce, J. P., D. L. Boone, S. Chai, R. E. Swain, T. Dassopoulos, S. Trettin, and A. Ma. 1998. IL-15 receptor maintains lymphoid homeostasis by supporting lymphocyte homing and proliferation. *Immunity* 9: 669–676.
36. Parrish-Novak, J., S. R. Dillon, A. Nelson, A. Hammond, C. Sprecher, J. A. Gross, J. Johnston, K. Madden, W. Xu, J. West, et al. 2000. Interleukin 21 and its receptor are involved in NK cell expansion and regulation of lymphocyte function. *Nature* 408: 57–63.
37. Kasaian, M. T., M. J. Whitters, L. L. Carter, L. D. Lowe, J. M. Jussif, B. Deng, K. A. Johnson, J. S. Witek, M. Senices, R. F. Konz, et al. 2002. IL-21 limits NK cell responses and promotes antigen-specific T cell activation: a mediator of the transition from innate to adaptive immunity. *Immunity* 16: 559–569.
38. Brady, J., Y. Hayakawa, M. J. Smyth, and S. L. Nutt. 2004. IL-21 induces the functional maturation of murine NK cells. *J. Immunol.* 172: 2048–2058.
39. Takaki, R., Y. Hayakawa, A. Nelson, P. V. Sivakumar, S. Hughes, M. J. Smyth, and L. L. Lanier. 2005. IL-21 enhances tumor rejection through a NKG2D-dependent mechanism. *J. Immunol.* 175: 2167–2173.
40. Funnell, A. P., K. S. Mak, N. A. Twine, G. J. Pelka, L. J. Norton, T. Radziewic, M. Power, M. R. Wilkins, K. S. Bell-Anderson, S. T. Fraser, et al. 2013. Generation of mice deficient in both KLF3/BKLF and KLF8 reveals a genetic interaction and a role for these factors in embryonic globin gene silencing. *Mol. Cell. Biol.* 33: 2976–2987.
41. Ding, L., Y. Ding, X. Kong, J. Wu, J. Fu, G. Yan, and H. Zhou. 2019. Dysregulation of Krüppel-like factor 12 in the development of endometrial cancer. *Gynecol. Oncol.* 152: 177–184.
42. Huang, C., H. Sun, Z. Wang, Y. Liu, X. Cheng, J. Liu, R. Jiang, X. Zhang, X. Zhen, J. Zhou, et al. 2018. Increased Krüppel-like factor 12 impairs embryo attachment via downregulation of leukemia inhibitory factor in women with recurrent implantation failure. *Cell Death Discov.* 4: 23.
43. Godin-Heymann, N., S. Brabetz, M. M. Murillo, M. Saponaro, C. R. Santos, A. Lobley, P. East, P. Chakravarty, N. Matthews, G. Kelly, et al. 2016. Tumour-suppression function of KLF12 through regulation of anoikis. *Oncogene* 35: 3324–3334.
44. Mak, C. S., M. M. Yung, L. M. Hui, L. L. Leung, R. Liang, K. Chen, S. S. Liu, Y. Qin, T. H. Leung, K. F. Lee, et al. 2017. MicroRNA-141 enhances anoikis resistance in metastatic progression of ovarian cancer through targeting KLF12/Sp1/survivin axis. *Mol. Cancer* 16: 11.
45. Xu, M., H. Jin, C. X. Xu, B. Sun, Z. Mao, W. Z. Bi, and Y. Wang. 2014. miR-382 inhibits tumor growth and enhance chemosensitivity in osteosarcoma. *Oncotarget* 5: 9472–9483.
46. Guan, B., Q. Li, L. Shen, Q. Rao, Y. Wang, Y. Zhu, X. J. Zhou, and X. H. Li. 2016. MicroRNA-205 directly targets Krüppel-like factor 12 and is involved in invasion and apoptosis in basal-like breast carcinoma. *Int. J. Oncol.* 49: 720–734.
47. Du, Y., Y. Chen, F. Wang, and L. Gu. 2016. miR-137 plays tumor suppressor roles in gastric cancer cell lines by targeting KLF12 and MYO1C. *Tumour Biol.* 37: 13557–13569.
48. Song, P., and S. C. Yin. 2019. Long non-coding RNA 319 facilitates nasopharyngeal carcinoma carcinogenesis through regulation of miR-1207-5p/KLF12 axis. *Gene* 680: 51–58.
49. Shin, Y., D. Y. Kim, J. Y. Ko, Y. M. Woo, and J. H. Park. 2018. Regulation of KLF12 by microRNA-20b and microRNA-106a in cystogenesis. *FASEB J.* 32: 3574–3582.
50. Ou, Y. H., P. H. Chung, F. F. Hsu, T. P. Sun, W. Y. Chang, and S. Y. Shieh. 2007. The candidate tumor suppressor BTG3 is a transcriptional target of p53 that inhibits E2F1. *EMBO J.* 26: 3968–3980.
51. Ren, X. L., X. H. Zhu, X. M. Li, Y. L. Li, J. M. Wang, P. X. Wu, Z. B. Lv, W. H. Ma, W. T. Liao, W. Wang, et al. 2015. Down-regulation of BTG3 promotes cell proliferation, migration and invasion and predicts survival in gastric cancer. *J. Cancer Res. Clin. Oncol.* 141: 397–405.
52. Liu, L., S. Liu, Q. Duan, L. Chen, T. Wu, H. Qian, S. Yang, D. Xin, Z. He, and Y. Guo. 2017. MicroRNA-142-5p promotes cell growth and migration in renal cell carcinoma by targeting BTG3. *Am. J. Transl. Res.* 9: 2394–2402.
53. Du, Y., P. Liu, W. Zang, Y. Wang, X. Chen, M. Li, and G. Zhao. 2015. BTG3 upregulation induces cell apoptosis and suppresses invasion in esophageal adenocarcinoma. *Mol. Cell. Biochem.* 404: 31–38.
54. Mao, D., L. Qiao, H. Lu, and Y. Feng. 2016. B-cell translocation gene 3 overexpression inhibits proliferation and invasion of colorectal cancer SW480 cells via Wnt/β-catenin signaling pathway. *Neoplasma* 63: 705–716.
55. An, Q., Y. Zhou, C. Han, Y. Zhou, F. Li, and D. Li. 2017. BTG3 overexpression suppresses the proliferation and invasion in epithelial ovarian cancer cell by regulating AKT/GSK3β/β-catenin signaling. *Reprod. Sci.* 24: 1462–1468.
56. Biron, C. A., and M. L. Tarrio. 2015. Immunoregulatory cytokine networks: 60 years of learning from murine cytomegalovirus. *Med. Microbiol. Immunol. (Berl.)* 204: 345–354.
57. Jensen, H., S. Y. Chen, L. Folkersen, G. P. Nolan, and L. L. Lanier. 2017. EBI3 regulates the NK cell response to mouse cytomegalovirus infection. *Proc. Natl. Acad. Sci. USA* 114: 1625–1630.
58. Lee, S. H., K. S. Kim, N. Fodil-Cornu, S. M. Vidal, and C. A. Biron. 2009. Activating receptors promote NK cell expansion for maintenance, IL-10 production, and CD8 T cell regulation during viral infection. *J. Exp. Med.* 206: 2235–2251.

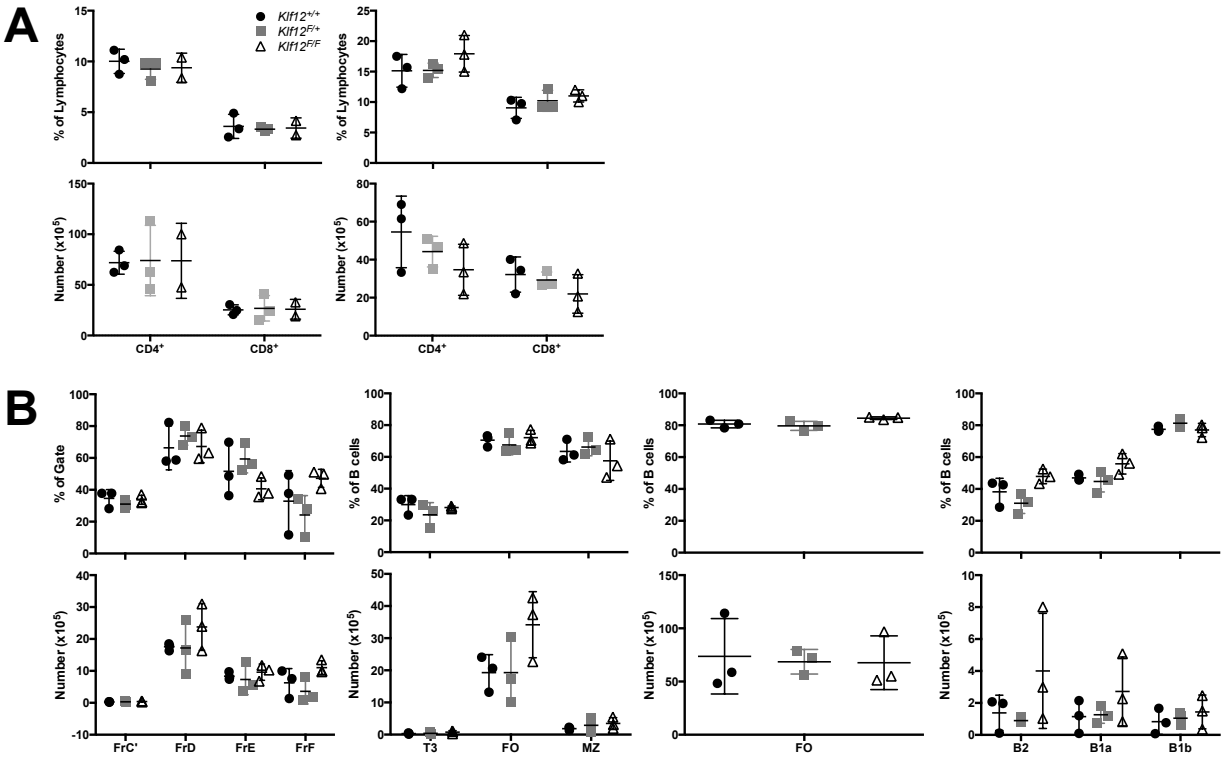

FIGURE 1. T and B cell development is normal in Klf12-deficient mice. **(A)** Percentages and total cell numbers of $CD4^+$ and $CD8^+$ T cells in the thymus (*left panels*) and in the spleen (*right panels*). **(B)** Percentages and total cell numbers of developmental B cell subsets in the BM (*left panels*), spleen (*second left panels*), lymph node (*second right panels*), and peritoneal cavity (*right panels*). Subsets in the BM are defined as FrC' pro-B cells: $CD19^+IgM^-B220^+CD43^+CD24^+$; FrD pre-B cells: $CD19^+IgM^-B220^+CD43^-$, FrE immature B cells: $CD19^+IgM^+B220^+AA4.1^+CD24^{hi}$; and FrF mature B cells: $CD19^+IgM^+B220^+AA4.1^-CD24^+$. Subsets in the spleen are defined as T3 (transitional stage 3) B cells: $IgM^+IgD^+CD19^+B220^+AA4.1^+CD23^+$; FO (follicular) B cells: $IgM^+IgD^+CD19^+B220^+AA4.1^-CD23^+$; and MZ (marginal zone) B cells: $IgM^+IgD^+CD19^+B220^+AA4.1^-CD23^-$. Subsets in the lymph node are defined as FO (follicular) B cells: $IgM^+IgD^+CD19^+B220^+AA4.1^-CD23^+CD21^+CD43^-$. Subsets in the peritoneal cavity are defined as B2 follicular B cells: $IgM^+IgD^+CD19^+CD43^-CD23^+CD5^-$; B1a B cells: $IgM^+IgD^+CD19^+CD43^-B220^+CD5^+$; and B1b B cells: $IgM^+IgD^+CD19^+CD43^+B220^+CD5^-CD11b^+$. Data are representative of 4 experiments (n = 3 mice/genotype/experiment).

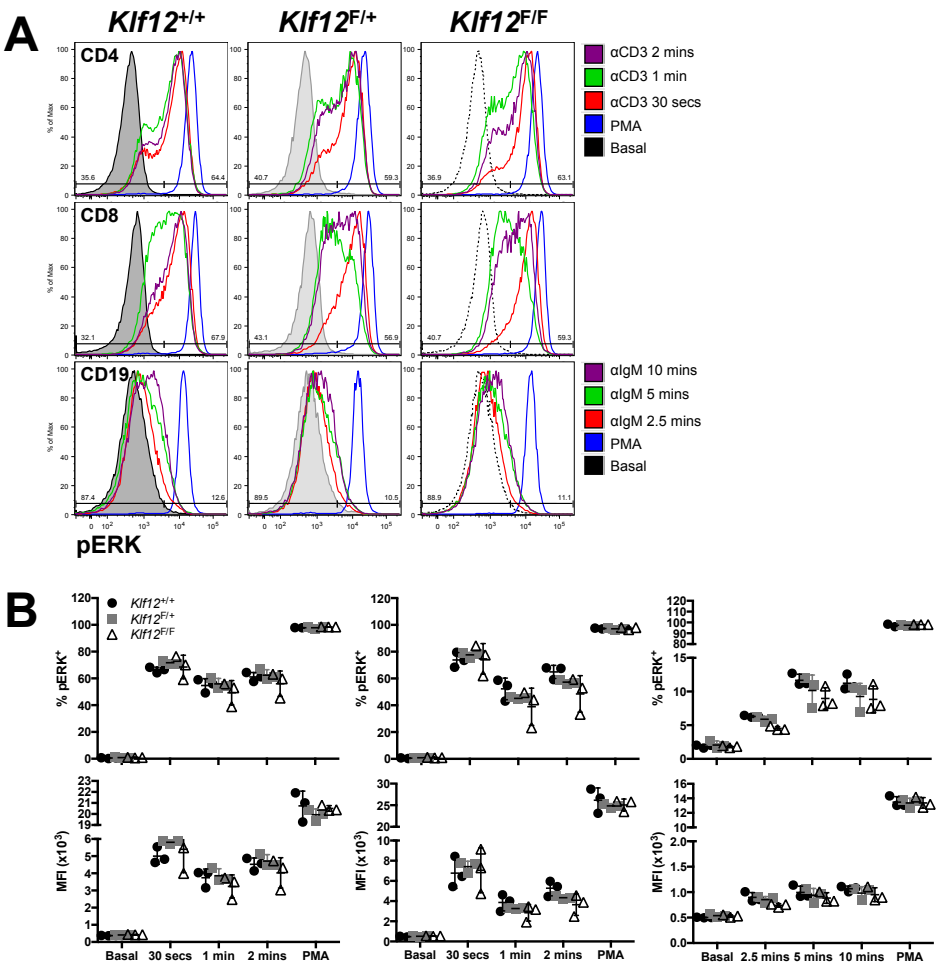

FIGURE 2. Upregulation of pERK is normal in Klf12-deficient T and B cells. **(A)** Representative histograms of pERK upregulation in lymph node CD4$^+$, CD8$^+$ T cells, and CD19$^+$ B cells from *Klf12*$^{+/+}$, *Klf12*$^{F/+}$, and *Klf12*$^{F/F}$ mice stimulated with anti-CD3 or anti-IgM. **(B)** Percentage and MFI of pERK in CD4$^+$ T cells (*left panels*), CD8$^+$ T cells (*middle panels*), and CD19$^+$ T cells (*right panels*). Data are representative of 4 experiments (n = 2-3 mice/genotype/experiment).

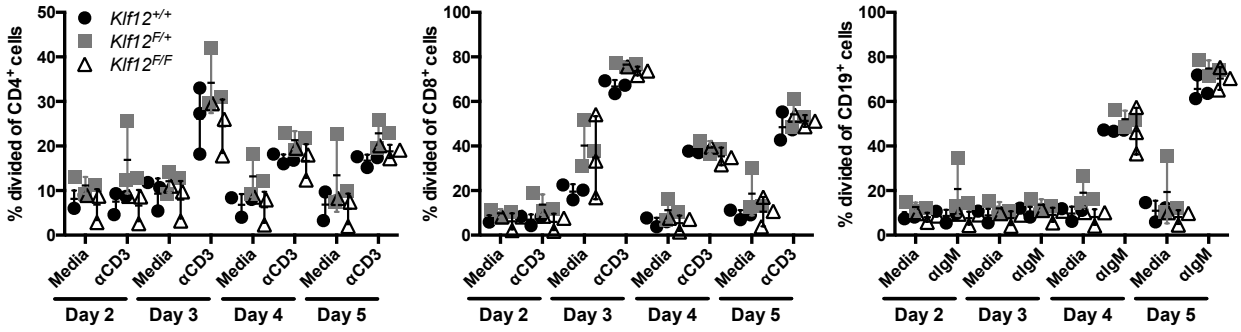

FIGURE 3. T and B cell proliferation is normal in Klf12-deficient mice. Proliferation of *Klf12*$^{+/+}$, *Klf12*$^{F/+}$, and *Klf12*$^{F/F}$ lymph node CD4^{+} T cells (*left panels*), CD8^{+} T cells (*middle panels*), and CD19^{+} T cells (*right panels*) after *in vitro* stimulation for 2-5 days with anti-CD3 and anti-IgM. Data are representative of 4 experiments (n = 2-3 mice/genotype/experiment).

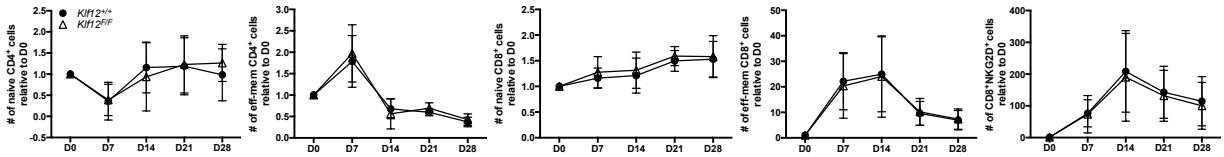

FIGURE 4. Normal numbers of Klf12-deficient T cells from MCMV-infected BM chimeric mice. Relative numbers of naïve ($CD44^{lo}CD62L^{+}$) $CD4^{+}$ T cells, effector-memory ($CD44^{hi}CD62L^{-}$) $CD4^{+}$ T cells, naïve ($CD44^{-}CD62L^{+}$) $CD8^{+}$ T cells, effector-memory ($CD44^{+}CD62L^{lo/+}$) $CD8^{+}$ cells, and MCMV-specific $NKG2D^{+}CD8^{+}$ T cells in the blood following MCMV infection. Data are representative of 4 experiments (n = 3-6 mice/experiment).